Discovering Levofloxacin Prototypes for Anti-inflammatory and Anti-bacterial Activity

M.Sc. Thesis

By

Shivani Vaja

BIOSCIENCES AND BIOMEDICAL ENGINEERING

INDIAN INSTITUTE OF TECHNOLOGY INDORE

May 2024

Discovering Levofloxacin Prototypes for Anti-inflammatory and Anti-bacterial Activity

A THESIS

Submitted in partial fulfillment of the

requirements for the award of the degree

Of

Master of Science

By

Shivani Vaja

BIOSCIENCES AND BIOMEDICAL ENGINEERING

INDIAN INSTITUTE OF TECHNOLOGY INDORE

May 2024

INDIAN INSTITUTE OF TECHNOLOGY INDORE

CANDIDATES'S DECLARATION

I hereby certify that the work which is being presented in the thesis entitled **'Discovering Levofloxacin Prototypes for Anti-inflammatory and Anti-bacterial Activity'** in the partial fulfilment of the requirements for the award of the degree of **MASTER OF SCIENCE** and submitted in the **DEPARTMENT OF BIOSCIENCES AND BIOMEDICAL ENGINEERING**, Indian Institute of Technology Indore, is an authentic record of my own work carried out during the period from July 2022 to May 2024. Thesis submission under the supervision of **Dr. Mirza S. Baig**, IIT Indore. The matter presented in this thesis has not been submitted by me for the award of any other degree of this or any other institute.

Signature of the student

Shivani Vaja

This is to certify that the above statement made by the candidate is correct to the best of my/our knowledge.

Signature of the supervisor of M.Sc. thesis

Dr. Mirza S. Baig

SHIVANI VAJA has successfully given her M.Sc. Oral Examination held on **9th May 2024**.

Signature of the supervisor of M.Sc. thesis

Date: 14-5-24

P.V. Kodgire

Convener, DPGC

Date: 20/05/24

ACKNOWLEDGEMENTS

Achievements of one's goal are not a single person's effort, but it is the pieces of advice, help, suggestions, and blessings of many people. So, it gives me immense pleasure to express my gratitude, regards, and acknowledgement to them.

I would like to express gratitude for this moment of accomplishment to my supervisor **Prf. (Dr.) Mirza Baig**, for providing me the golden opportunity of working in their lab. I got to learn many new things while working on this project. Their continuous guidance, timely advice, scientific approach, and support always helped in moving forward. I am indebted to them for always finding time between their busy schedules to discuss my results and clear my doubts. Without their guidance and persistent help, this project would not have been possible within the limited time frame.

I would also like to thank the Director, **Prof. Suhas S. Joshi**, for allowing me to be coursework a part of this prestigious institute. Also, I would humbly like to express my gratitude to all the faculty members of BSBE who taught me various courses during course work and encouraged me to pursue my career further in research. I would like to thank **Prof. Amit Kumar** (Head, Department of Biosciences and Biomedical Engineering) and **Prof. Prashant Kodgire** (DPGC), **Dr. Parimal Kar** (Course coordinator) for their continuous support in various aspects during the M.Sc. journey.

I would like to express my heartful thanks to **Mr. Pawan Kumar Yadav,** for his valuable lessons and support and to lab members **Mr. Kundan Solanki, Mr. Khandu Wadhonkar, Mr. Pramod Patidar, Mr. Rajat Atre, Mr. Shivmuni Sarup, Ms. Shreya Bharti, Ms. Yusra Sayyed, Ms. Yashika Sajida,** and **Mr. Lateefur Rahman Khan** for all their valuable lessons, helping during all the experiments.

I would like to express my deep gratitude to project collaborators, **Prof. Prabha Garg (NIPER Kolkata), Mr. Tanmay Vyas and Mr. Vineet Diwarkar**. I would like to thank **Dr. Ghanshyam, Kinny Pandey** and for their valuable discussion and time, at the SIC facility of IIT Indore. Nevertheless, I would like to thank all my batchmates for keeping me motivated, energetic and enthusiastic for every upcoming hurdle, and my friends **Ms. Mili Patel**, **Ms. Mitsu Solanki**, and **Ms. Broti Mitra** who are like my family away from home.

I would like to express my deep gratitude to the source of my life, my parents, **Mr Bharat Bhai Vaja, Mrs Heenaben Vaja**, and my eldest brother and sister-in-law**, Mr Ankur Vaja, Mrs Disha Vaja**, and youngest brother, **Mr Dipesh Vaja,** for their unconditional love, care, support and without them, I would not be here where I am today. Last but not least, I would like to thank Almighty God for granting me strength and health and all others who knowingly or unknowingly helped me in this journey.

Shivani Vaja

Dedicated

To

My Parents

and

My Family

Abstract

Sepsis is a chronic inflammatory disease involving other diseases as well. Different stages of sepsis lead to organ dysfunction and eventually death. Sepsis is recognized as an uncontrolled and dysregulated host immunological response to any infection or damage. A multitude of injuries or diseases can result in sepsis. The pathophysiology of sepsis is still unknown. Thus, a therapeutic approach for sepsis should be highly potential. Sepsis is caused by polymicrobial species such as bacteria, fungi, viruses or even parasites. The research claimed may be a therapeutic drug medication that targets major inflammatory immune responses. In sepsis, causing microorganisms are also prime important as an exaggerated immune response. In this project, we are targeting our novel drug molecules against the causes of the disease as well as immune response targets. Thus, we majorly target sepsis. Our dual drug targets, DNA Gyrase, and TIRAP will be inhibited by a novel drug molecule simultaneously. Whoever suffers from either bacterial sepsis or immunomodulatory sepsis, will be cured by one therapeutic drug only. Our therapeutic approach will try to treat sepsis more extensively. Despite the unknown pathophysiology of sepsis, Sepsis can be cured.

LIST OF PUBLICATIONS

1. Integrative Strategies: An In-Depth Analysis of Combination or modified Therapies Leveraging CAR-T/M/NK Cells for Targeted types of cancer for therapeutics, **Shivani Vaja**, Shubhi Khandelwal, Chaitali Vora, **Mirza Baig.**

2. Effect of Reactive Oxygen, Nitrogen, and Sulfur Species on Signaling Pathways in Atherosclerosis, Kundan Solanki, Evgeny Bezsonov, Alexander Orekhov, Suraj P Parihar, **Shivani Vaja**, Alexander G. Obukhov, **Mirza S. Baig**

   Vasc. Pharmacol IF: 5.7, 107288 (155) 2024

Contents

LIST OF FIGURES

Chapter 1

Chapter 3

LIST OF TABLES

ABBREVIATIONS

AP-1	Activator Protein-1
cDNA	Complimentary DNA
DMEM	Dulbecco's Modified Eagle Medium
DMSO	Dimethyl Sulfoxide
EDTA	Ethylenediamine tetra acetic acid
FBS	Fetal Bovine Serum
GAPDH	Glyceraldehyde 3-phosphate dehydrogenase
IL	Interleukin
LPS	Lipopolysaccharide
cDNA	Complimentary DNA
ANOVA	Analysis of Variance
qRT-PCR -	Quantitative Reverse Transcription Polymerase Chain Reaction
TNF-α	Tumor Necrosis Factor Alpha
FDA	Food and Drug Administration

NOMENCLATURE

ml	milliliter
mM	millimolar
Ng	nanogram
µl	microliter
µM	Micro-molar
°C	Degree centigrade

Chapter:1

1. Introduction

Sepsis is a chronic inflammatory disease that is a major cause of morbidity and mortality, it can lead to organ failure and disruption and eventually to death (Gyawali, Ramakrishna & Dhamoon 2019). Sepsis, septic shock, and systemic inflammatory immune response syndrome can lead to burns, trauma or several associated inflammatory-related diseases. There are several infectious causes of sepsis such as bacteria, fungi, viruses or even parasites (Huang, Cai & Su 2019). The epidemiology and pathogenicity of sepsis are still unknown as there are changes in incidence and causing pathogens organisms over time (Martin 2012). Sepsis is also dependent on several factors such as age, sex, race and ethnicity. Sepsis is majorly associated with organ dysfunction, as it is caused by infectious agents, but it is not the infection that kills the people, it is the host's immune response to fight the infection and may cause fatal organ failure (Gyawali et al. 2019).

The incidences and causes of sepsis are more important as compared to the downstream of disease (Martin 2012). Sepsis is caused by polymicrobial species, consisting of bacteria, fungi, viruses, and parasites.

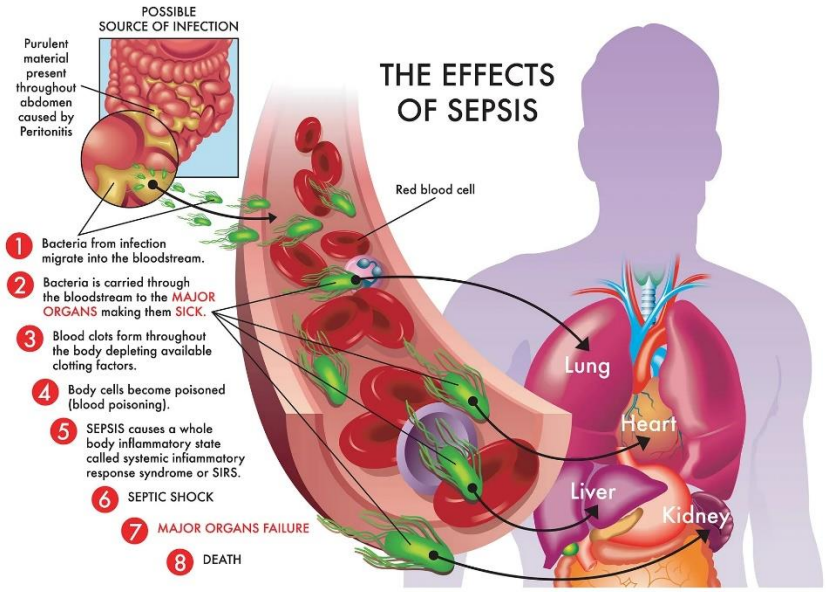

Figure: 1.1. Inflammatory response in sepsis. (Google source: https://www.micoope.com)

Sepsis is potentially a fatal organ dysfunction syndrome that results from uncontrolled and dysregulated host immunological response to any infection or damage (Sygitowicz & Sitkiewicz 2020). A multitude of injuries or disease can result in sepsis.

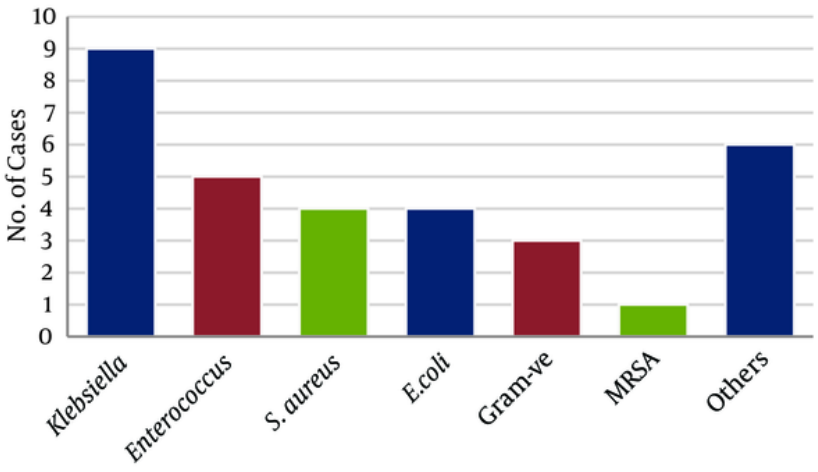

Figure:1.2. Frequency of Isolated Organisms in Sepsis Patients (Pawar et al. 2016)

The pathogen or cytokines are first released into bloodstream by diseased or injured tissue. The blood contains a large range of cells that might induce inflammation, such as neutrophils, natural killer cells and, most notably, macrophages (Chen et al. 2018). Infections, cytokines, and inflammatory cells that spread to other organs, where they cause inflammation. If this reaction continues for an extended period, sepsis, a condition characterized by persistent inflammation and a variety of abnormalities develops. When persistent inflammation is not treated for an extended period, an illness called severe sepsis develops (Nedeva, Menassa & Puthalakath 2019). This causes a variety of organ dysfunctions. This can be detected by a variety of signs and symptoms, including an increase in heart rate, high blood sugar, decrease in urine, increase in breathing rate and confusion. Furthermore, if left untreated, it results in septic shock, a cardiovascular malfunction (Gyawali et al. 2019). As the disease progresses, three major conditions might be noticed. SIRS is characterized by a high or low body temperature, a fast pulse, and an elevated respiratory rate (Loots et al. 2021). Sepsis involves the presence of two symptoms as well as bodily infection. Severe sepsis is distinguished by the presence of hypotension or hypoperfusion in addition to sepsis. At this time, we can witness low blood platelet count, breathing issues, decreased urine production, stomach discomfort, and changes in mental health. The presence of hypotension and an increase in lactate levels indicate septic shock. It is the most lethal stage, with a mortality rate of more than 60% (Gyawali et al. 2019).

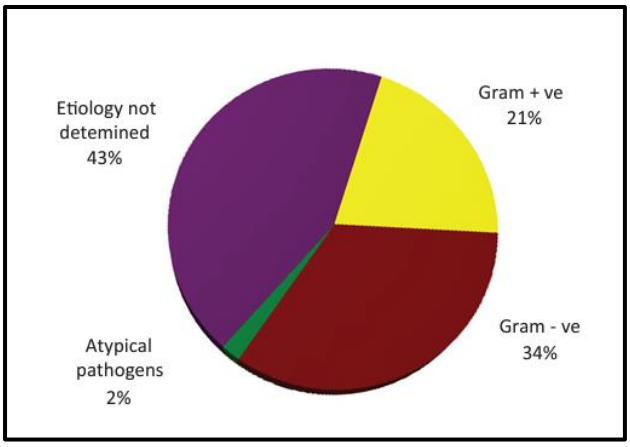

Figure 1.3. Types of pathogens involved in etiology of septic patients (Pawar et al. 2016)

A total of 1352 causative pathogens, including 571 gram- positive bacteria, 709 gram-negative bacteria, and 35 fungi, were identified in the 928 patients. A polymicrobial infection with two or more causative pathogens was present in 200 patients. Sepsis is found across the world, but it is most common in South America, Africa, and the Indian subcontinent. There is also a mortality rate of 40-80%(Rudd et al. 2018). Several medicines are available to eliminate the pathogen, provide supportive care, and assist the host in recovering from continuous organ damage caused by chronic inflammation. Antimicrobial therapy can be performed by either delivering a broad-spectrum antibiotic or administering various antibiotics. Ventilation should be included in supportive care to ensure an appropriate supply of oxygen. Erythrocyte transfusion is an option in extreme circumstances. Antibodies can suppress inflammatory mediators such as cytokines and endotoxins (LPS) (Leekha, Terrell & Edson 2011). One is the suppression of inflammatory mediators such as cytokines and endotoxins (LPS) by antibodies or other mechanisms such as insulins, which boosts LDL cholesterol. Despite the availability of these medications, the death rate remains high. As the unknown pathophysiology of sepsis, approach can be proposed(Tsalamandris et al. 2019).

1.1. Antibacterial Drug target therapy

To address the upcoming problem with antibiotic resistance, there are various ways means, including increased surveillance to map the course of resistance spread and development of rapid diagnostic methods to ensure early selection of suitable therapeutics. However, the rate of discovery of developable novel antibacterial agents has been decreasing, as it followed many years of focused pursuit of new antibiotics with little success (Duque-Villegas et al. 2020). Antibiotic resistance Era increases in the 1980s and 1990s, starting with MRSA, the pharmaceutical and research industry looked for new ways to attack the problem. One direction that proved productive was reevaluation and development of previously discovered antibiotics targeting Gram-positives and improved this discovery field with the help of bioinformatics and Computation biology (Duque-Villegas et al. 2020).

DNA Gyrase is found in eubacterial DNA synthesis machinery. It is a member of the type II subfamily of DNA topoisomerases (McKie, Neuman & Maxwell 2021). In DNA synthesis, helicase ensures the unwinding of double-stranded DNA producing the strain on DNA strands.

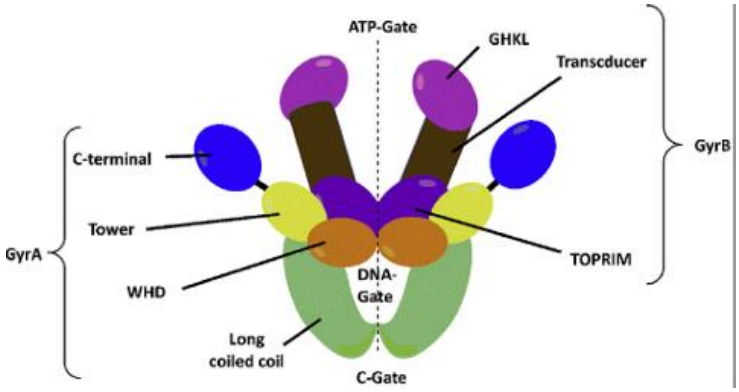

Figure 1.4. Structure of bacterial DNA gyrase. DNA gyrase with two subunits each of GyrA and GyrB. The winged-helix domain (WHD), long domain, tower

domain and variable C-terminus are all subunits of GyrA. Conversely, the GyrB subunit is comprised of only three domains i.e. GHKL (gyrase, Hsp90, histidine kinase, MutL), ATP transducer and TOPRIM (topoisomerase/primase). The ATP gate is localized within the GHKL domain, whilst the DNA gate and C-gate are confined to the long coiled-coil domain and TOPRIM domains of DNA gyrase respectively(Dighe & Collet 2020).

It is a heterotetrametric structure consisting of two subunits- GyrA and GyrB. Eukaryotic topoisomerase also consists of two subunits- ParA and ParC(Spencer & Panda 2023). Topoisomerases are associated with helicase enzymes to make sure to relieve the strain on the strands and thus maintain the topological state of DNA. This enzyme machinery is important for molecular activities such as replication and transcription (Spencer & Panda 2023).

Topoisomerase II enzyme machinery involves double-stranded breaks in duplex DNA. Three key structures play an important role: N-gate, DNA gate (also G-gate) and C-gate. At the DNA gate, DNA binds with the enzyme and both strands are cleaved and pulled apart by a conformational change (Champoux 2001).

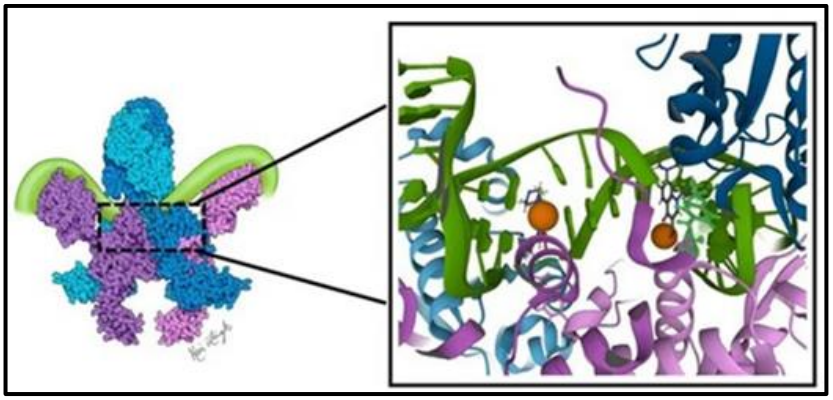

Figure:1.5. Binding of quinolones to DNA gyrase and replication machinery of Gyrase with DNA (Champoux 2001)

The class of fluoroquinolone antibacterial drugs target DNA Gyrase, it binds reversibly to DNA gyrase at the interface between enzyme and DNA near the active site, thus inhibiting a broad spectrum of bacteria. DNA Gyrase is a validated drug target for the therapeutic approach of multidrug-resistant tuberculosis (Chopra et al. 2012). Fluoroquinolones act by stabilizing the gyrase–DNA cleavage complex. Fluoroquinolones inhibit DNA gyrase functionality by blocking dsDNA annealiation after cleavage(Cozzarelli 1980). Quinolones have both bacteriostatic and bactericidal actions. The stabilization of gyrase–DNA complexes stalls replication forks and slows bacterial growth. At higher concentrations, quinolones become bactericidal as chromosomes are fragmented, and cells rapidly die (Anderson & Osheroff 2001). In fluoroquinolone-resistant bacteria, mutations appear at the quinolone binding site of DNA gyrase, and are located at amino acids Tyr122, Ser83 and Asp87 (Wohlkonig et al. 2010). This GyrA subunit domain is also known as quinolone resistance determining regions (QRDR) (Onseedaeng & Ratthawongjirakul 2016). DNA Gyrase is used as target by many therapeutics such as quinolones, coumarins, indoles, azoles, pyrraloamides and Gyr-A and B inhibitors.

1.2. Anti-inflammatory drug target therapy

TIRAP, also known as MyD88-adaptor Like (MAL), is an adaptor protein molecule associated with the activation of host immune signaling (Belhaouane et al. 2020). TIRAP interacts with downstream signaling kinase molecules such as PKCδ, BTK, MyD88, and p85α activating the inflammatory immune signaling mechanism. The innate immune system recognizes microbial pathogens through receptors, including Toll-like receptors (TLRs), which identify pathogen-associated molecular patterns (PAMP) (Deguine & Barton 2014). Upon ligation of most TLRs with their respective ligands (PAMP), TIRAP-mediated signaling machinery leads to

the phosphorylation of kinase protein and there is nuclear translocation of p38 and NF-κB leads to the activation of pro-inflammatory cytokine genes (Rajpoot et al. 2021). More recent studies show that TIRAP not only acts as a bridging protein between TLR4/ 2 and MyD88, but also propagates transduction of downstream signaling events(Lannoy et al. 2023). The ability of TIRAP to interact and collaborate with several signaling molecules in a context-dependent manner means this protein is a major regulator of cell signaling. TIRAP is an important drug target for an anti-inflammatory drug molecule (Rajpoot et al. 2021).

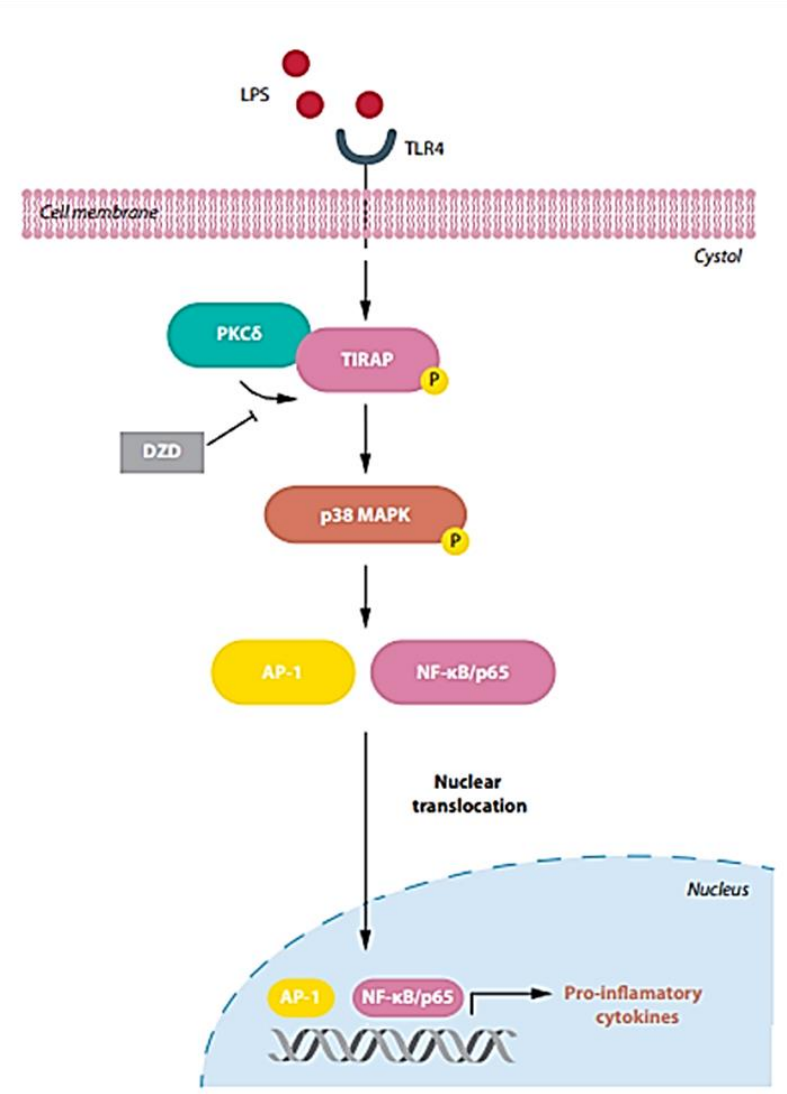

Figure: 1.6. Stimulation of TLR by LPS leads to the activation of signaling pathway involving p38 MAPK, PKCδ, BTK, p38, and nuclear translocation of NF-κB/p65 activates the pro-inflammatory cytokine genes leads to the generation of inflammatory immune response. Dorzolamide (DZD) is well known inhibitor for TIRAP suppressing the pro-inflammatory immune response signaling.

1.3. Objectives

1. *In vitro* analysis of compounds

• To check the Anti-inflammatory activity of compounds:

Pro-inflammatory cytokines levels in RAW cells, Phosphorylation of TIRAP adaptor protein in immunoblot, Interaction of PKCδ and BTK in confocal microscopy.

• To check the anti-bacterial activity of compounds: Bacterial assays: Zone of inhibition test (Kirbeabaur test), Minimum inhibitory concentration, Minimum bactericidal concentration, MTT assay and time kill study.

2. *In vivo* analysis of compounds

• To check the Anti-inflammatory activity of compounds: Serum and tissue pro-inflammatory cytokine level. Arrangement of cells in tissues in H &E staining. Interaction of BTK and PKCδ in Immunohistochemistry.

• To check the anti-bacterial activity of compound

1.4. Motivation

The transition from the traditional 'one drug/one target' approach to the 'one drug/multi-target' or 'multi-pharmacology' model marks a significant evolution in drug discovery and development strategies (Boyd et al. 2021). This shift recognizes the complexity of diseases, which often involve interconnected pathways and networks rather than isolated targets. Leveraging multiple targets with a single drug offers the potential for more effective treatments by addressing the multifaceted nature of many diseases. Factors driving this transition include advances in systems biology, the practice of drug repurposing, and the desire to reduce side effects and resistance. While multi-target approaches hold promise for discovering new treatments, they also present challenges such as off-target interactions and

unexpected side effects. Therefore, thorough pharmacological profiling and safety assessments are crucial. Overall, the move towards multi-target drug discovery reflects a more holistic understanding of disease mechanisms and treatment strategies, offering potential benefits in terms of efficacy, safety, and the exploration of novel therapeutic avenues.

Sepsis is a chronic inflammatory disease involving other diseases as well. There are different stages of sepsis that leads to organ dysfunction and eventually death. Sepsis is recognized as an uncontrolled and dysregulated host immunological response to any infection or damage. A multitude of injuries or diseases can result in sepsis. The pathophysiology of sepsis is still unknown. Thus, a therapeutic approach for sepsis should be highly potential. Sepsis is caused by polymicrobial species such as bacteria, fungi, viruses or even parasites. The research claimed may be a therapeutic drug medication that targets major inflammatory immune responses. In sepsis, causing microorganisms are also prime important as an exaggerated immune response. In this project, we are targeting our novel drug molecules against the causes of the disease as well as immune response targets. Thus, we majorly target sepsis. Our dual drug targets, DNA Gyrase, and TIRAP will be inhibited by a novel drug molecule simultaneously. Whoever suffers from either bacterial sepsis or inflammatory sepsis will be cured by one therapeutic drug only. Our therapeutic approach will try to treat sepsis more extensively. Despite the unknown pathophysiology of sepsis, Sepsis can be cured.

The aim of this project is the multitude of targets for broader therapeutics for sepsis. *In silico* analysis of levofloxacin similar compounds has been performed in computational software. *In silico* approach is usually used to screen the compounds based on computational prediction.

The resultant drug molecule analysis has been done *in vitro* and *in vivo* experiments will be done. The finalized drug molecules will target the two-

drug target receptors and show dual activities: Anti-bacterial and anti-inflammatory activity.

Chapter: 2

Materials and Methods

2.1. Protein and ligand molecule's structure Retrieval and Preparation

The crystal structure of Topoisomerase II from Mycobacterium tuberculosis (PDB Id- 5BTG) with resolution-2.50 Å, and TIR domain-TIRAP (PDB Id-3UB2) with resolution- 2.4 Å structure were obtained from RCSB Protein data bank (www.rcsb.org). The crystal protein structures possessed a resolution around 2.00 Angstrom by the X-ray diffraction method. Using the Discovery studio BIOVIA, the ligand or inhibitor and water molecules were eliminated from protein structure prior to docking. Missing polar hydrogens and kolmann charges and other atomic charges were adjusted in Auto-dock auxiliary (ADT) tool version 4.2 (Morris et al. 2009). The protein structures were finally saved in PDB and PDBQT format. The levofloxacin similar library - 3D drug molecule conformers and levofloxacin and dorzolamide were retrieved in SDF format from PubChem (www.pubchem.ncbi.nlm.nih.gov). Open Babel was used to change the file format. All two control drug molecules along with levofloxacin similar 3D conformers drug library and three drug targets saved as in PDBQT format.

2.2. Molecular Docking

Auto dock Vina and Schrodinger GLIDE module software's were utilized to analyze protein-drug interactions. Blind docking was performed and for Gyrase, protein grid box centered at (X-108, Y-76, Z-88), and TIRAP protein grid box centered at (X-40, Y-36, Z-34) were prepared and saved the output grid file in text format. A docking program was run on

AutoDock/Vina using Command prompt which employs an iterated local search global optimizer(Handoko et al. 2012). Docking was performed on alternate basis where levofloxacin drug library docked with Gyrase and the docked interactions of Protein and drug molecules were analyzed in BIOVIA Discovery studio. Further, resultant drug molecules with best binding score compared with FDA-approved drug (Levofloxacin) and then the resultant ligand molecules with best binding energy were docked with second drug target- TIRAP and compared the resultant drug molecules with Dorzolamide as anti-inflammatory drug control agent and best drug molecules were analyzed for dual activities. Discovery BIOVIA studio and UCSF chimera were used for protein-drug interactions and further analyzed.

2.3. Molecular dynamic simulations

To assess the binding profiles of ligands with their respective proteins, molecular dynamic simulations were conducted. A total of 12 systems were constructed using the system builder provided by Schrodinger software package(Madhavi Sastry et al. 2013), Maestro. 2022: Schrödinger, LLC, New York, NY.] Topoisomerase-II (T1) from Mycobacterium tuberculosis complex (comprising 5 compounds and a control), and TIR domain-TIRAP (T3) complex (with 5 compounds and a control). To stabilize the simulation systems, Na+ counter-ions were introduced, maintaining a salt concentration of 0.15 M NaCl. The systems were enclosed in an orthorhombic box, and the simple point charged (SPC) water model, along with the OPLS4 force field, (Lu et al. 2021) was employed for the simulations. The model system, held at a temperature of 310 K and a pressure of 1.01325 bar, underwent energy minimization and equilibration in the NPT ensemble. During the simulations, system pressure and temperature were maintained using the Martyna–Tobias–Klein barostat (Nosé 1984; Hoover 1985; Cho, Joannopoulos & Kleinman 1993) and

Nose–Hoover Chain thermostat, [Evans, D.J. and B.L. Holian, the nose–hoover thermostat. The Journal of chemical physics, 1985. 83(8): p. 4069-4074.] respectively. All the systems were simulated for the time period of 100 ns with default relaxation protocol involving predefined minimization and molecular dynamic steps to ensure system relaxation before the production run. Subsequently, trajectories were analyzed using the Simulation Interactions diagram module of Desmond and the Maestro interface of Schrodinger. MMGBSA calculations were performed overall 100 ns trajectory using thermal_mmgbsa.py (Lyne, Lamb & Saeh 2006) script provided by the Schrodinger.

All molecular dynamics calculations were executed using the Desmond package of Schrodinger 2021-3 on Ubuntu 22.04.3 LTS (Intel® Xeon(R) W-3265 CPU @ 2.70GHz × 48).]

2.4. Physicochemical properties and ADMET prediction

The physicochemical properties according to Lipinski's rule, Pharmacokinetic and toxicity prediction were done using two online platforms: Pkcsm (https://biosig.lab.uq.edu.au/pkcsm/) and ADMETlab 2.0. (https://admetmesh.scbdd.com/) Drug molecules canonical SMILE retrieved from Pubchem and used for ADMET prediction.

2.5. BMDM Isolation and culture

Mice were sacrificed by cervical dislocation, and the femur bone was obtained for bone-marrow-derived macrophage (BMDM) culture. Flush the bones with lymphocyte medium using a 5-mL syringe and a 25-gauge needle. BMDM cells were grown in Dulbecco's modified Eagle's medium (11965118; Gibco, NY, USA) supplemented with heat-inactivated 10% fetal bovine serum (10270106; Gibco) and 100U/ml penicillin and

100µg/ml streptomycin (15140122; Gibco). For BMDM, 20% of L929 conditioned medium was added to complete the medium, and fresh medium was replenished on the third day of the culture. To achieve maximum confluency, all cells were cultured in a humidified incubator with 5% CO2 at 37◦ up to 6 days. Then the cells were treated with 1000 ng LPS and novel drug at varying dosages. The media were discarded prior to treatment and cells were treated for 12 hours.

Mouse macrophages: RAW 264.7 was purchased from the National Centre for Cell Science (NCCS), Pune, India. These were cultured in DMEM (Dulbecco's minimal essential medium) supplemented with 10% heat inactivated Fetal Bovine Serum (FBS) and 1% antibiotic (penicillin and streptomycin).

2.6. RNA isolation and Real-Time Quantitative PCR

RT-PCR works based on the fluorescent reporter assay where the intensity of a fluorescent signal is generated by an intercalating dye during the amplification of target sequence and the number of PCR cycle upto which fluorescent signal is noticeable is called CT value. The CT value can be compared after subtracting and normalizing with the housekeeping gene CT value and the one cycle decrease can be related to the double of target sequence. This can be expressed as $2^{-\Delta CT}$. The values can be plotted, and unknown targets can be interpolated.

For the present study, the treated BMDM cells and RAW 264.7 treatment was terminated using RNAiso Plus reagent (Takara Bio Inc.) and placed at -80°c overnight. Total RNA was isolated from cultured BMDM cells by RNAiso Plus reagent (Takara Bio Inc.) according to manufacturer's instructions. The concentration and purity of extracted RNA were determined by the ratio of absorbance readings at 260 nm and 280 nm

(A260/A280). Total RNA (1 µg) was reverse transcribed (RT) using the HUWEL cDNA Synthesis Kit according to the manufacturer's specifications. Real-time PCR was performed using SYBR® Select Master Mix (Applied Biosystems) in StepOnePlus Real-Time PCR Systems (AppliedBiosystems). Briefly, the reaction conditions consisted of 0.5 µl of cDNA and 0.2 µM primers in a final volume of 20 µl of supermix. Each cycle consisted of denaturation at 95 °C for 15 s, annealing at 57.5 °C for 5 s and extension at 72 °C for 10 s, respectively. The primer sets used are described in **Table: 5.1.**

2.7. MTT assay

RAW 264.5 cells were grown at 37 °C in a 5% CO_2 environment using Dulbecco's modified Eagle medium (DMEM) supplemented with 10% (v/v) FBS (fetal bovine serum) and 1% antibiotics penicillin/streptomycin, 10,000 U mL^{-1}. The viability of the cells (RAW 264.5) was checked in the presence of novel drug by a conventional MTT assay. The cells at the density of 1×10^4 were seeded in 96-well plates and grown for 24 h. Subsequently, the media were replaced by fresh media containing novel drug. The novel drug was checked for the concentration ranging from 1 to 200 µM mL^{-1} in duplicates. The wells containing only media were taken as control. After 24 h, the media was replaced with fresh media containing MTT of 5 mg mL^{-1}. The purple-colored formazan crystals were dissolved using 100 µL of DMSO per well, and the absorbance was recorded at 570 nm using a UV-plate reader. The percentage cell viability was calculated using formula.

2.8. Immunofluorescence

In 12-well culture plates, 1*104 cells were cultivated on coverslips (18 mm in diameter). Overnight, all cells were grown in serum-free DMEM to allow them to synchronize. Cells were given drug treatment for 15 minutes prior

to LPS treatment. Lipopolysaccharide (LPS- 1000 ng/ml) were applied to cells for the stated times. Cells were then washed with 1X PBS one time after the medium had been aspirated. The cells were fixed for 20 minutes at room temperature with freshly prepared 4% paraformaldehyde and then after washing they were permeabilized for 10 minutes with 0.1% Triton-X 100. Cells were blocked with 5% BSA in 1X Tris-buffered saline, 0.1% Tween®20 detergent (TBST) for 90 minutes, after fixation and permeabilization, followed by an overnight staining procedure at 4°C using primary antibodies with 1:200 dilution in blocking buffer. The cells were stained with secondary antibodies with dilution 1:500 in 1X TBST for an hour at room temperature after being washed with TBST three times for 5 minutes each. Nuclear counterstaining along with mounting is carried out in accordance with the manufacturer's instructions using DAPI containing mounting media. The Olympus confocal laser scanning microscope (FV100) was used to study the coverslips after mounting them onto glass slides with mounting fluid. Images were taken at 100X magnification. The list of primary antibodies and secondary antibodies are listed in **Table-5.2**.

2.9. Hemolysis Assay

Collected healthy human blood in heparin or sodium citrate tubes and immediately centrifuge at 1700× g for 5 min. Avoided using needles above 23 G to minimize pre-analyte hemolysis. Removed the supernatant by aspiration and washed the erythrocytes by adding 2 mL of PBS pH~7. Centrifuged at 1700× g for 5 min. Repeated the washing step three times or until the supernatant was clear. Removed supernatant and diluted the erythrocyte pellet 1:100 in PBS pH~7 to obtain a 1% erythrocyte suspension. Mix 50 µL of the 1% erythrocyte suspension with 50 µL of test compound in a 96-well polypropylene plate with conical wells (PCR plate). Used 10% Triton X-100 (Sigma-Aldrich, Saint-Louis, MO, USA, T8787) as a positive control and PBS (pH~7) as a negative control in identical volumes as test

drug compound. Incubated the plate at 37 °C for 60 min. Centrifuged the plate at 1700× g for 5 min. Transfer 50 µL of the supernatant to a transparent, flat-bottom 96-well plate and measure absorption at 405 nm in a plate reader.

2.10. Determination of Anti-microbial activity of novel drug

The antimicrobial activities of the drug samples were evaluated through the determination of the minimum inhibitory concentration (MIC) by the broth dilution method in culture broth (https://doi.org/10.1038/nprot.2007.521). For the antibacterial assays, the compounds were dissolved in DMSO: NFW (1:9) (5 mg/ml) to make main stock. Further dilutions were prepared at the required quantities of 10, 20, 30, 40, 50, 60, and 70 µg/ml concentrations. The minimum inhibitory concentration (MIC) values were determined using the method of twofold serial dilutions (https://doi.org/10.1046/j.1469-0691.2003.00790.x). The Nutrient Broth, which contained tested samples and controls, was inoculated with approximately 5×10^5cfu/ml of actively dividing bacterial cells. The cultures were incubated for 24 h and 48 h at 30°C on a metabolic rotary shaker (220 rev/min), and the growth was monitored visually and spectrophotometrically (at 600 nm). To ensure that the solvent had no effect on bacterial growth, a control test was also performed containing inoculated broth supplemented with only DMSO: NFW at the same dilutions used in our experiments and found inactive in culture medium. The MIC was defined as the lowest concentration required to arrest the growth of the bacteria at the end of 24 h of incubation. The MBC was determined by subculturing a 0.1-ml volume of the medium drawn from the culture tubes after 48 h on Nutrient Agar and incubated further for bacterial growth. The growth was scored for relative numbers of bacterial colonies. The lowest concentration of the antimicrobial agent causing negative growth (fewer than three colonies) was considered the MBC.

Chapter:3

Results and Discussion

3.1 Molecular Docking study

In the current study, a set of levofloxacin similar compounds library was selected to carry out the studies to assess their multitarget potential against sepsis-causes such as bacteria, fungal pathogens, and hosts-immune response. To examine the possibility of binding with multiple targets, we have selected three targets- A bacterial drug target- DNA Gyrase, and an inflammatory drug target protein-TIRAP and screened the compounds by molecular docking method along with their known inhibitors as the control or reference compounds such as Levofloxacin for Gyrase, and Dorzolamide for TIRAP. The binding energy obtained for the 5 hit drug compounds with two targets along with reference compound is tabulated in **Table-1**. The results obtained from the molecular docking studies are compared with the already reported- FDA drug compounds as reference molecules that inhibit three targets.

3.1.1. Docking studies of Levofloxacin similar library compounds with the DNA Gyrase

DNA Gyrase is found in eubacterial DNA synthesis machinery. It is a member of the type II subfamily of DNA topoisomerases. The crystal structure of DNA topoisomerases consists of DNA Gyrase subunit A (503 sequence length) and subunit B (253 sequence length). An anti-bacterial drug- Levofloxacin library consists of 842 drug molecule (Chemical vendor availability) structures retrieved from PubChem library. Molecular docking of these anti-bacterial drug molecules against DNA Gyrase target in

docking platform- Auto dock vina. The molecular docking of these drug molecules was performed using an FDA-approved anti-bacterial agent-Levofloxacin as positive control. Out of 842 molecules, 55 were showing a high dock score (Gibbs free binding energy) compared to the levofloxacin (Dock score: -17.9). Based on virtual screening in Auto-dock Vina, these 55 compounds were binding DNA topoisomerase and predicted to have anti-bacterial activity.

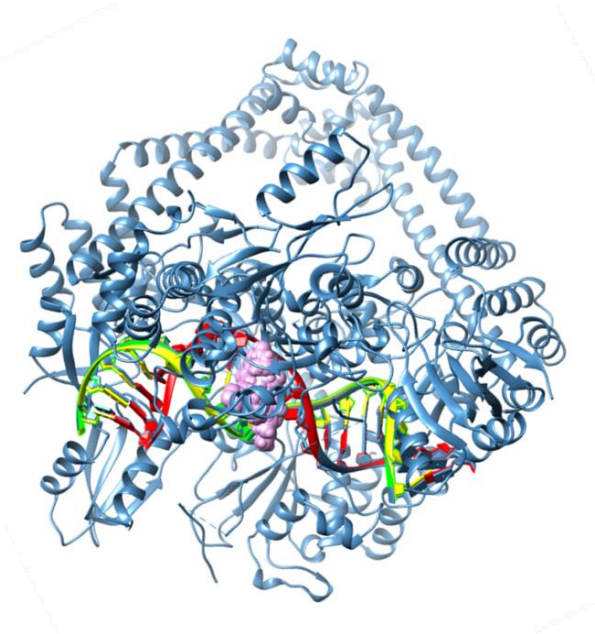

Figure:3.1. Interaction of 5 drug molecules with an Anti-bacterial drug target-DNA Gyrase in DNA binding segment region. All these compounds bind at the same binding pocket in reference to levofloxacin as control. The pink doted structure represents a group of drug molecules that interact with the DNA binding domain of gyrase at DNA gate. Blue, yellow and green colored structures represent DNA strand.

3.1.2. Docking studies of the compounds with TIRAP

TIRAP is an important drug target for an anti-inflammatory drug molecule (Rajpoot et al., 2023). Molecular docking was performed with an anti-

inflammatory drug target-TIRAP in Auto-dock and Schrodinger Glide module -docking platforms taking an anti-inflammatory drug molecule-Dorzolamide as a positive control. Out of 55 compounds, 5 compounds showed higher binding energy and lowered dock score as compared to dorzolamide and common in both platforms. These 5 drug molecules were also analyzed based on presence of critical residues respectively with their targets and positive controls. The dock score of these 5 compounds were high as the binding energy of these compounds with anti-bacterial, and anti-inflammatory target receptors- Gyrase, and TIRAP, respectively. These 5 drug molecules are summarized with the binding score against their targets along with respective reference molecules. It suggests the novel 5 drug molecules' binding affinity is high compared to respective positive controls in **Table :1**

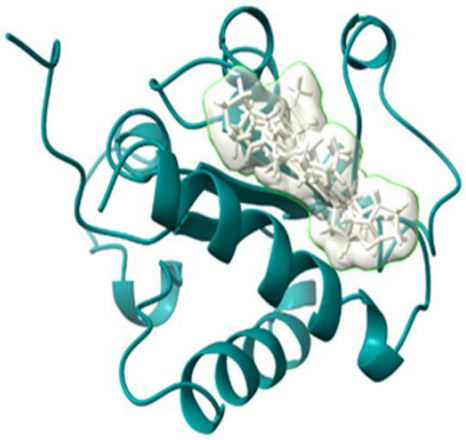

Figure:3.2. Interaction of 5 drug molecules with TIRAP at same binding pocket of PKCδ and BTK. All these compounds bind at the same binding pocket in reference to Dorzolamide as control. Cyan blue colored structure represents the domain structure of TIRAP, and grey colored transparent structure represents drug molecules.

Table:1 Five drug molecules are summarized with the binding score (Red colored) and interacting residues against their targets along with respective reference molecules.

Compounds PubChem CID	Gyrase	TIRAP
C-1	483, 461, 482, 10, 128, 90, 11, 15, 14, 500, 501 **-18.1**	216 174 169 168 194 176 177 195 212 197 196 208 211 215 **-8**
C-2	500, 501, 14, 15, 482, 11, 128, 91, 90, 10, 483 **-17.9**	215 216 175 168 169 174 176 195 212 197 208 198 211 **-7.2**
C-3	501, 500, 461, 482, 483, 128, 10, 11, 15, 14,90 **-18.5**	219 216 169 175 177 176 195 196 197 198 208 211 215 212 **-7.8**
C-4	483, 482, 128, 10, 90, 11, 15, 14, 500 **-18.1**	215 211 208 197 196 195 212 176 175 177 168 174 169 **-7.8**
C-5	90, 128, 10, 461, 483, 482, 500, 14, 15 **-18.5**	169 168 175 174 177 176 196 197 212 195 208 211 215 **-7.8**
Levofloxacin	461 483 501 500 482 15 14 91 90 128 10 11 **-17.9**	
Dorzolamide		168 169 216 213 212 142 174 175 176 177 197 196 195 H 194 **-5.7**

3.2. Structural stability analysis by Molecular dynamic simulation

Molecular dynamic studies were conducted on the top complexes to evaluate their stability and binding free energy. Stability was assessed through Root Mean Square Deviation (RMSD) and Radius of Gyration (Rg) analyses applied to the entire trajectory. Simultaneously, the evaluation of binding free energy was conducted using Molecular Mechanics/Generalized Born Surface Area (MMGBSA) analysis.

3.2.1. Simulation Analyses of DNA Topoisomerase

The RMSD analyses indicate that all the complexes exhibit stability over time, with minimal fluctuations observed after 40 ns. The control group shows an average RMSD of 2.38 ± 0.24 Å, while the complex with compound one displays an average RMSD of 2.08 ± 0.22 Å. Complexes with compounds 2-5 exhibit RMS deviations close to that of the control. Similar observations were noted in the Radius of Gyration (Rg) analyses. Except for the complex with compound 1, all complexes demonstrate a consistently stable Rg, as detailed in **Table: 2** Both RMSD and Rg analyses affirm the overall stability gained by all complexes during the simulation period.

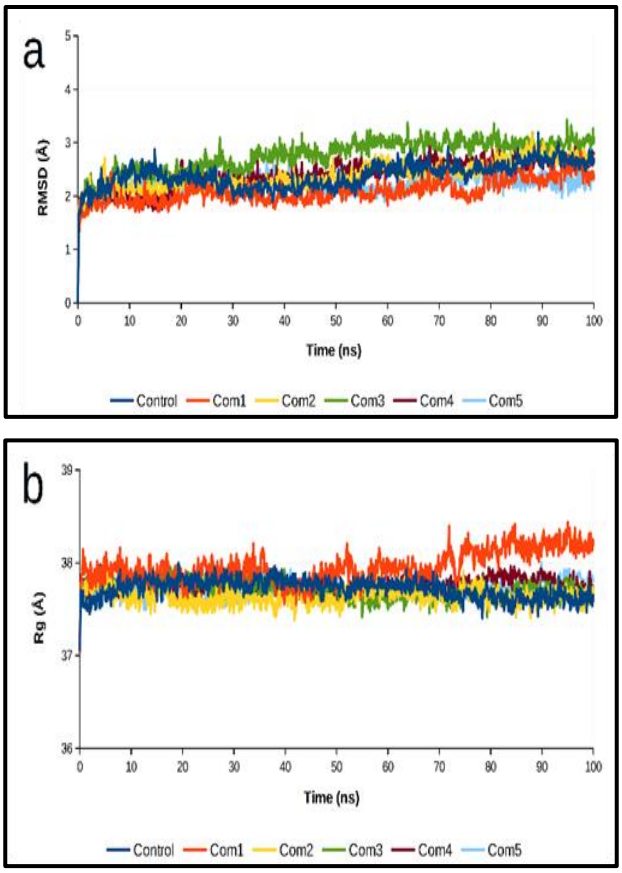

Figure: 3.3. RMS Deviation (a) and Radius of gyration (b) of the target 1 with different compounds.

Throughout the simulation, the control compound consistently forms two water bridges with Pro124 (C) and establishes hydrogen bonds with Asp461(B) and Ser462(B). The hydrogen bond with Asp461 appears to be a stable interaction, observed 78% of the time. On the other hand, compound 1 forms one water bridge with Gln277(A) and two hydrogen bonds with Ser340(A) and Gln336(A). Compound 2 engages in multiple interactions, including one hydrogen bond with Glu501(D) observed for 94% of the total simulation time, suggesting a prominent interaction. Additionally, it forms a Pi-cation interaction and another hydrogen bond with Arg482(D) and Arg128(A), respectively.

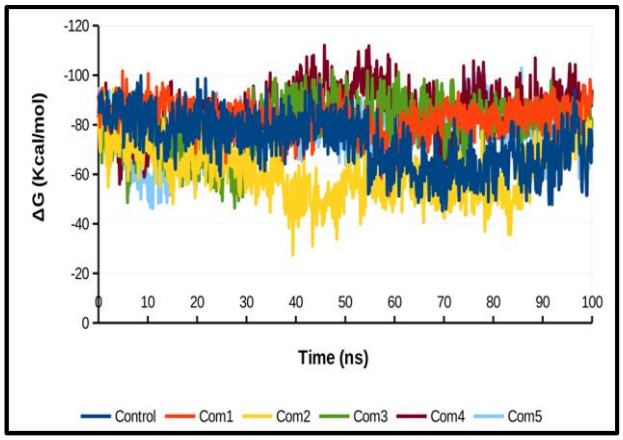

Figure: 3.4. MMGBSA analyses of the Target 1 with different compounds.

Further analysis by MMGBSA results demonstrates that all complexes exhibited better binding affinity than control complex. The complex with compound 4 displayed the lowest average ΔG bind of -84.85 ± 9.94 kcal/mol, followed by compound 1 (-82.35 ± 6.51 kcal/mol) and 3 (-79.63 ± 10.15 kcal/mol), respectively.

3.2.2. Simulation Analysis of TIRAP

In the case of target 2, the RMSD of the control initially exhibits deviations, but stability is achieved after 25 ns, with an average RMSD of 2.29 ± 0.29 Å. The complex with compound 4 demonstrates the minimum RMSD deviation, with an average of 2.30 ± 0.16 Å. The complex with compound 1 initially shows more deviation, likely due to initial fluctuations in the structure, but stabilizes after 40 ns. Complexes with compounds 1 and 2 exhibit more deviation throughout the simulation compared to other complexes.

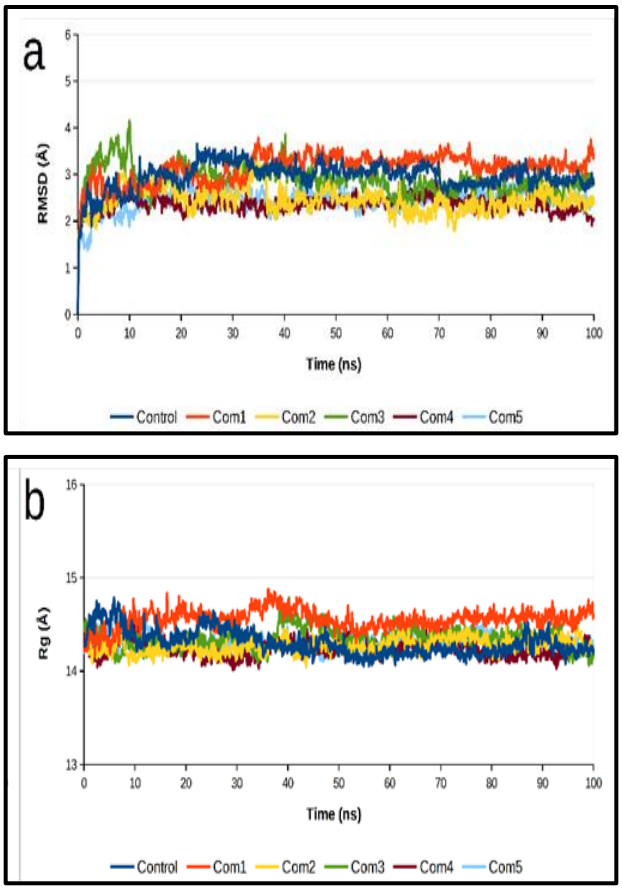

Figure:3.5. RMS Deviation (a) and Radius of gyration (b) of the target 2 with different compounds.

The Radius of Gyration (Rg) for target 3 complexes shows very small fluctuations throughout the 100 ns simulation. MMGBSA analysis of the complexes associated with target 3 indicates that the control complex has an average ΔG bind of -23.26 ± 7.09 kcal/mol, which is significantly higher compared to the complexes with compounds 2-5. These complexes exhibit average ΔG bind values ranging from -45 kcal/mol to -48 kcal/mol, as presented in **Table: 2**.

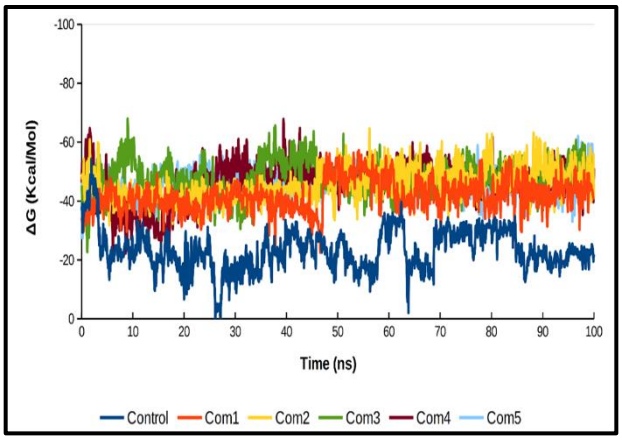

Figure: 3.6. MMGBSA analyses of the Target 2 with different compounds.

In comparison to the other two targets, target 2 exhibits a relatively poor interaction profile. The control of target 3 does not show any prominent interactions. However, compound 3 and compound 5 form one Pi-Pi interaction each, with Tyr195(A) and Tyr216(A), respectively. Compound 4 forms several water bridges and one Pi-Pi interaction, while compound 2 shows one hydrogen bond, as illustrated in **Figure: 3.6**.

Table:2. Simulation summary

Complex	**RMSD (Å)**	**Rg (Å)**	**MMGBSA (Kcal/mol)**
T1_Control	2.38 ± 0.24	37.72 ± 0.1	-72.98 ± 10.72
T1_Com1	2.09 ± 0.23	37.96 ± 0.17	-82.35 ± 6.51
T1_Com2	2.38 ± 0.27	37.63 ± 0.09	-60.78 ± 10.65
T1_Com3	2.76 ± 0.31	37.71 ± 0.1	-79.63 ± 10.16
T1_Com4	2.4 ± 0.28	37.76 ± 0.08	-84.86 ± 9.94
T1_Com5	2.23 ± 0.18	37.72 ± 0.08	-76.2 ± 9.5
T2_Control	6.41 ± 0.72	25.37 ± 0.38	-37.15 ± 4.68
T2_Com1	5.34 ± 0.82	25.31 ± 0.45	-41.39 ± 5.3

T2_Com2	5.65 ± 0.87	25.25 ± 0.37	-66.9 ± 9.44
T2_Com3	5.82 ± 0.95	25.38 ± 0.29	-55.89 ± 5.08
T2_Com4	4.96 ± 0.44	25.56 ± 0.15	-56.77 ± 6.39
T2_Com5	4.23 ± 0.66	25.43 ± 0.37	-48.81 ± 6.4
T3_Control	2.96 ± 0.29	14.3 ± 0.13	-23.27 ± 7.1
T3_Com1	3.13 ± 0.3	14.56 ± 0.1	-41.86 ± 5.39
T3_Com2	2.46 ± 0.27	14.27 ± 0.08	-45.91 ± 5.65
T3_Com3	2.89 ± 0.3	14.35 ± 0.11	-48.01 ± 6.16
T3_Com4	2.36 ± 0.17	14.24 ± 0.09	-46.75 ± 6.88
T3_Com5	2.45 ± 0.25	14.32 ± 0.07	-46.05 ± 4.45

3.3. Physicochemical properties study based on the Lipinski's rule.

The physicochemical properties of the compounds were studied to predict the pharmacokinetics of the drug by Lipinski's rule. The guidelines for an orally active drug according to the Lipinski's rule are (i) molecular weight (MW) < 500 Daltons, (ii) octanol-water partition coefficient (clogP) < 5, (iii) polar surface area (PSA) < 150 Å2, (iv) number of hydrogen bond donors (HBD) < 5, (v) number of hydrogens bond acceptors (HBA) < 5 and (vi) Number of rotatable bonds (RB) < 10. The calculated values for the same for the compounds that are shown to possess high activity after simulation studies are tabulated in Table: 2 and the result showed that the compounds follow Lipinski's rule except 11222571 and 461411 This indicates that the compounds have the potential for drug-like activities.

3.4. Prediction of ADMET profiling

ADMET- Absorption, distribution, metabolism, excretion, and toxicity strategies used in the development of novel medicines. These 5 drug molecules were also examined. The significance of *in silico* pharmacokinetics and screening of our 5 hit drug molecules in comparison to the selected control medications cannot be overstated. Three controls, Anti-bacterial control agent, anti-fungal control agent and anti-inflammatory control agent- Levofloxacin, and Dorzolamide, respectively.

The pharmacokinetic study reveals that these 5 drug compounds are predicted to be absorbed easily via human intestine. These compounds show good skin permeability, and were P-glycoprotein substrates, meaning that these compounds are actively eliminated from cells via P-glycoprotein through an ATP-binding cassette transporter for drug excretion. They are poorly distributed in the brain via the blood brain barrier and unable to permeate the central nervous system. These compounds are predicted to be non-carcinogenic, with no AMES toxicity and none of the compounds show inhibitors of CYP enzyme family. These compounds may cause hepatotoxicity like FDA approved control drug molecules. *In vitro* and *In vivo* studies are needed to confirm the pharmacokinetics and toxicity of these drug molecules. Predicted ADMET properties are tabulated in **Table:3.**

Table:3. ADMET pharmacokinetic prediction properties summarized in table including absorption, metabolism, distribution, excretion, and toxicities of these finalized 5 drug molecules along with respective control drug molecules.

Parameters		Levofloxacin	Dorzolamide	C-1	C-2	C-3	C-4	C-5
Physicochemical properties	M.W	361.37	324.44	352.365	374.412	389.402	345.301	403.429
	Log P	1.544	0.612	3.85	2.39	2.45	3.3704	2.98
	Rotatable bond	2	3	3	2	3	3	4
	Acceptor bond	6	6	4	6	5	4	5
	Donor bond	1	2	1	1	1	2	1
Absorption	Water Solubility	-3.179	-2.418	-3.271	-4.176	-3.078	-3.067	-3.084
	$CaCo_2$ Solubility	1.365	0.407	1.024	1.243	1.26	1.249	1.223
	Intestinal absorption	97.397	79.546	97.782	97.6	94.865	96.042	94.067
	Skin permeability	-2.735	-3.454	-2.735	-3.097	-2.735	-2.735	-2.735
Distribution	Fraction unbound	0.577	0.45	0.376	0.256	0.552	0.099	0.55
	BBB Permeability	-0.792	-0.838	-0.613	-0.711	-0.101	-0.663	-0.094
	CNS permeability	-3.054	-3.134	-2.036	-2.887	-2.443	-2.937	-2.426
Metabolism	CYP2D6 Substrate	No	No	No	No	No	No	No
	CYP2D6 inhibitor	No	No	No	No	No	No	No
Excretion	Total clearance	0.414	0.07	0.475	0.643	0.483	0.214	0.673
Toxicity	AMES Toxicity	No	No	No	No	No	No	No
	Hepatotoxicity	Yes	Yes	Yes	Yes	Yes	Yes	Yes
	Skin sensitization	No	No	No	No	No	No	No

3.5. MTT assay

In the era of toxicity or side effects of emerging novel drug, determination of the toxicity of novel compound is critically important. Here, a comparative analysis of the cytotoxic action of drug has been performed against RAW 264.7 cell line. After 24 hours of incubation with various concentrations of drug ranging from 1 µM to 400 µM, cell viability has been determined. No significant changes were observed between the control cells and with low dose (10–100 µM) treated cells. Cell death was not observed in this range while experiments were done up to 100 µM as the required dose of drug is less than the 100 µM.

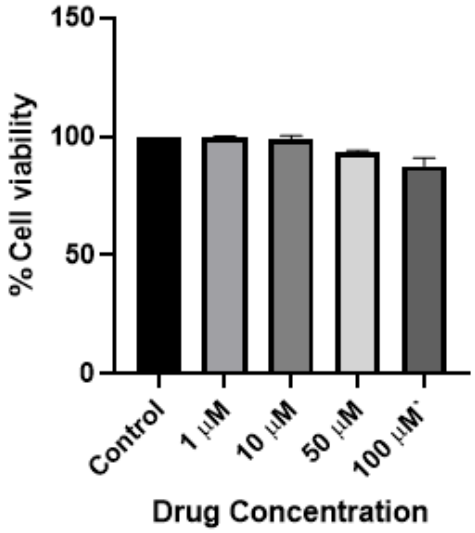

Figure: 3.7. MTT assay results showing cell viability under different drug concentrations ranging from 1 µM to 100 µM up to 24 h. Results are represented as a mean of 2 readings ±SD. Statistical analysis was performed using Graph Pad Prism 4 software and one way ANOVA test. Statistical significance was assumed for p-values o0.05: *p o 0.05, **p o 0.01, ***p o 0.001.

3.6. Hemolysis Assay

For the hemolysis assay, we used 1% washed erythrocytes from the human blood samples, incubated for 60 min at 37°C with different concentrations of drug ranges from 100 µM to 400 µM and positive control (10% Triton X) as detergent for it is crucial that the positive control sample in fact contains cells that are hemolyzed as completely as possible, so that the maximum amount of hemolysis is well defined., and negative control (phosphate buffered saline, PBS, pH 7) controls, after which the optical density (OD) was measured at 405 nm to detect the amount of hemoglobin released. In this assay, we can speculate that drug is not cytotoxic in the context of RBC lysis and release of hemoglobin. After treating with 100 µM drug concentration, there was slightly hemolysis was observed. At 400 µM concentration, 50% hemolysis was observed.

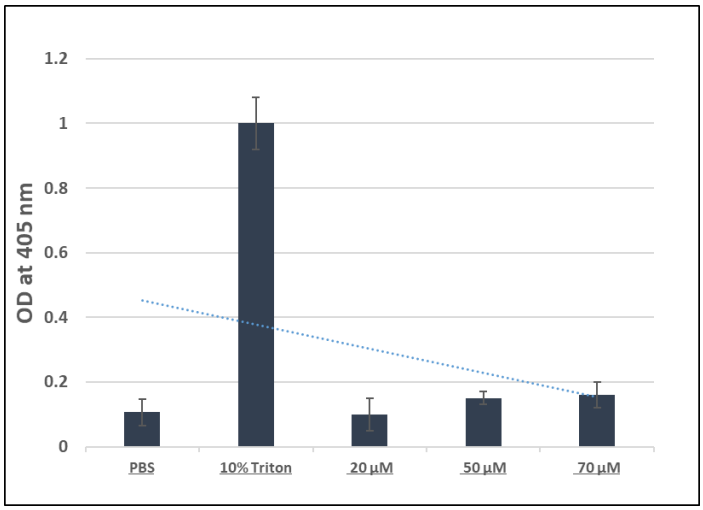

Figure: 3.8. OD measurements at 405 nm (Y-axis) of free hemoglobin in 1% erythrocyte solutions taken from human, incubated for 60 min at 37°C with PBS (negative control), 10% Triton X-100 (positive control), drug concentrations (20 µM, 50 µM, 70 µM). Average values from two experimental replicates, each containing two technical replicates, are presented with error bars (SD) included in plot.

3.7. Exploring Drug for Anti-inflammatory activity

3.7.1. Expression of Pro-inflammatory cytokines

The expression of pro-inflammatory cytokines is an endpoint marker to evaluate the response of inflammatory signaling pathways and plays an important role in regulating the host immune response. Therefore, the impact of several LPS-induced, inflammatory responses generated through LPS stimulation leads to the upregulation of pro-inflammatory cytokine genes. BMDM were treated with LPS (1 µg) and drug at two conditions- 10 µM and 50 µM for 12 hours. RAW 264.7 were treated with LPS (1 µg) and drug at two conditions- 10 µM and 50 µM for 4 hours The 12-hour BMDM treated cells and 4-hour RAW-264.7 treated cells were terminated and then subjected to RNA isolation and cDNA synthesis and then real time PCR. Interestingly, drug significantly suppressed the expression of TNF-α, IL-1β, and IL-6 on primary BMDMs, respectively(**Figure:3.9.**). The relative expression of TNF-α and IL-1β is much more significantly reduced in 10 µM and 50 µM drug treated cells. This pro-inflammatory cytokine data suggests that the drug may exhibit anti-inflammatory activity.

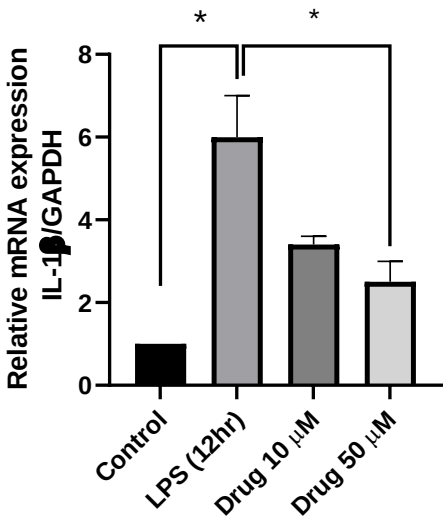

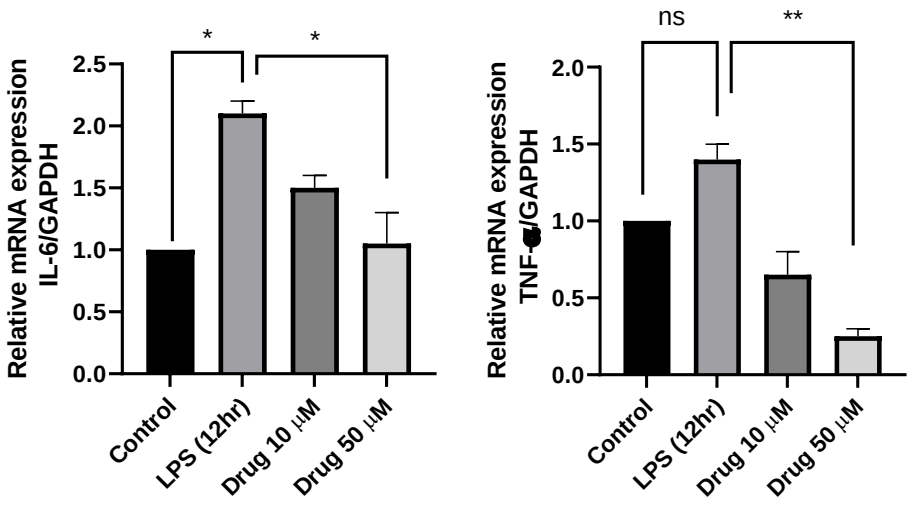

Figure:3.9. Effect of CD on proinflammatory cytokine expression of LPS induced mouse bone marrow derived macrophages. The total RNA was isolated and 1µg from each sample was used for single-stranded cDNA preparation as per manufacturer's instruction. Prepared cDNA was used as the template DNA for real-time PCR and relative mRNA expression of pro-inflammatory cytokines was estimated with respect to GAPDH; Relative expression of (i) TNF-α, (ii) IL-1 β, and (iii) IL-6. Data are mean ± SEM (n=3). All data are representative of three independent experiments; all are presented as mean ± SD. P values were determined by Student's t-test; *$p < 0.05$, **$p < 0.005$.

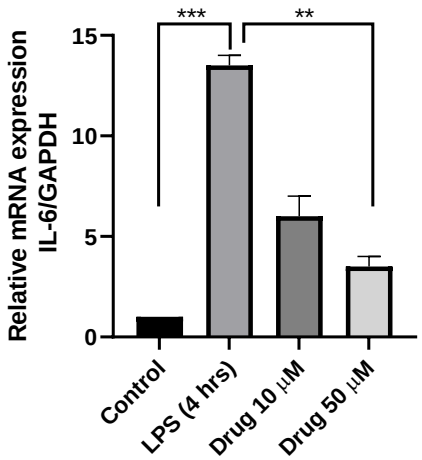

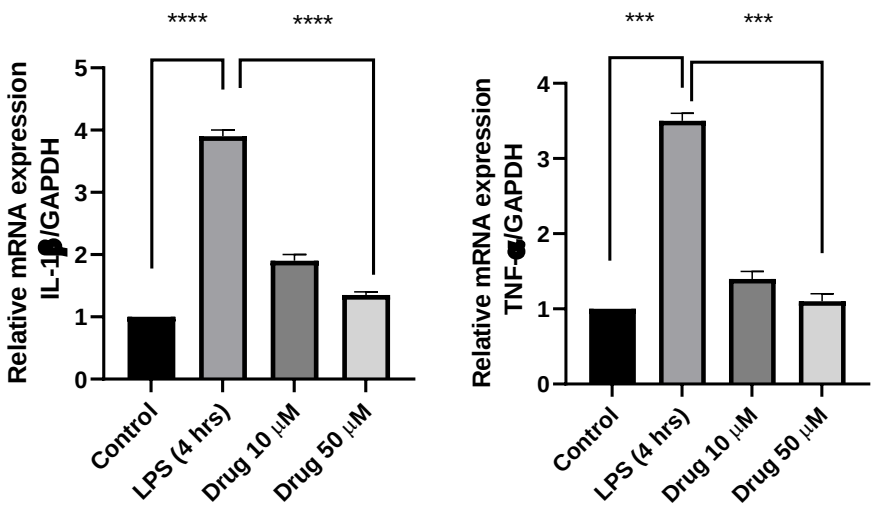

Figure:3.10. The effect of drug on proinflammatory cytokine expression of LPS induced RAW 264.7 treated for 4 hrs. The total RNA was isolated and 1µg from each sample was used for single-stranded cDNA preparation as per manufacturer's instruction. Prepared cDNA was used as the template DNA for real-time PCR and relative mRNA expression of pro-inflammatory cytokines was estimated with respect to GAPDH; Relative expression of (i) TNF-α, (ii) IL-1 β, and (iii) IL-6. Data are mean ± SEM (n=3). All data are representative of three independent experiments; all are presented as mean ± SD. P values were determined by Student's t-test; *p < 0.05, **p < 0.005.

3.7.2. Drug inhibits TIRAP phosphorylation in LPS-stimulated macrophages.

Upon LPS stimulation of macrophages, TLR4 and TIRAP are phosphorylated by kinases. Tyrosine phosphorylation of the TIRAP TIR domain is crucial for its downstream activity. Because the *in-silico* analysis suggested that drug 5 interacts with TIRAP, it was predicted that Drug 5 treatment would decrease TIRAP phosphorylation. Both Y86 and Y106 within the TIRAP TIR domain represent crucial phosphorylation sites for PKCδ. Phosphorylation of TIRAP at Y86 (p-TIRAP) showed a modest

increase over time, and this was significantly decreased at post-LPS treatment in drug-treated RAW 264.7 macrophages. No changes in total TIRAP levels were observed. However, the downregulation of TIRAP phosphorylation at LPS activation strongly suggests that drug 5 decreases TIRAP activation by blocking its interaction to PKCδ and subsequent phosphorylation by this kinase. Therefore, these data suggest that novel drug 5 interacts with TIRAP and might inhibit the downstream signaling pro-inflammatory signaling.

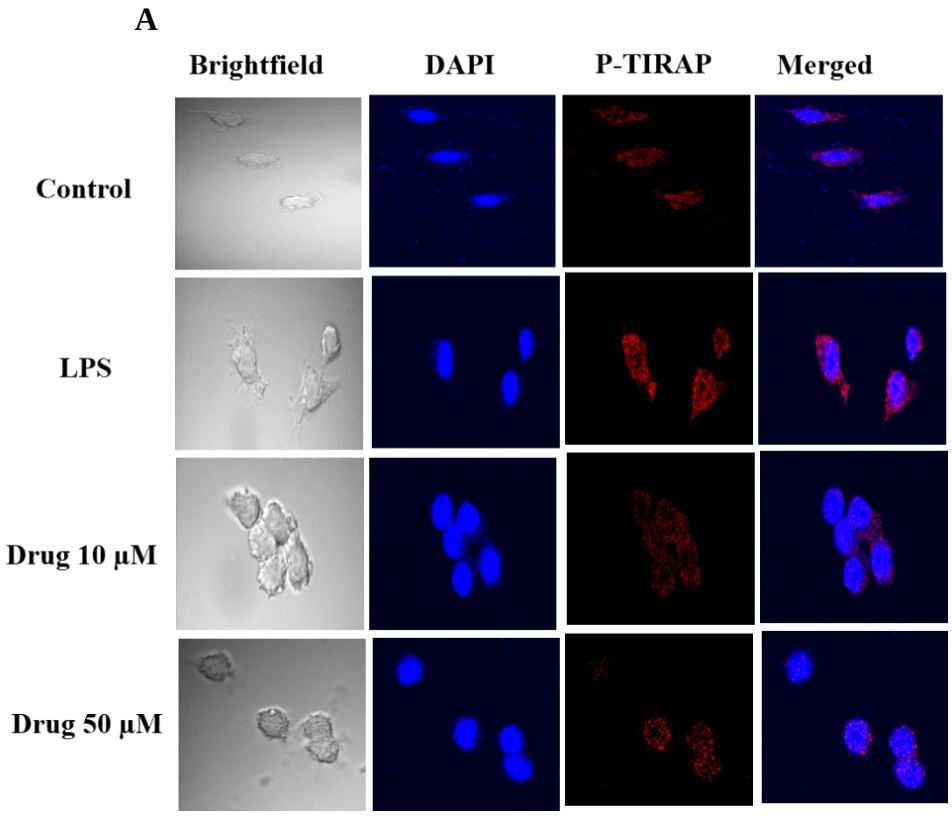

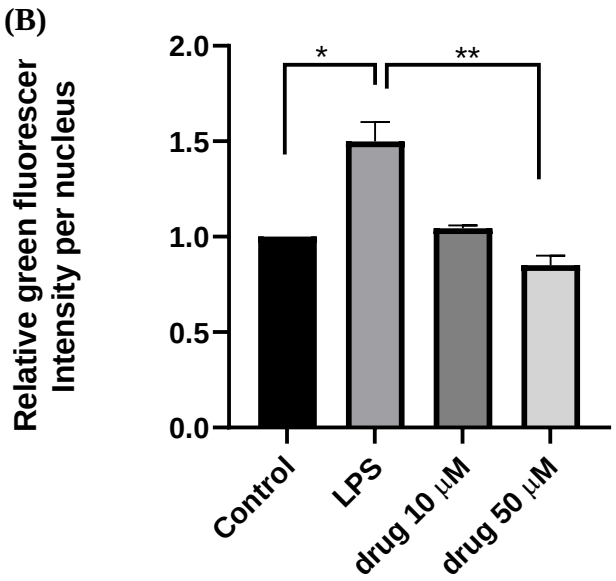

Figure: 3.11. Drug 5 inhibits LPS-induced phosphorylation of TIRAP in RAW 264.7 macrophages. **(A)** Immunofluorescence confocal microscopy of p-TIRAP in RAW 264.7 macrophages. RAW 264.7 macrophages were treated with an anti-p-TIRAP antibody to determine the level of p-TIRAP (red). Nuclei were counterstained with DAPI (blue) and slides were visualized using confocal microscopy. Merged images of the red and blue fluorescence are shown. Original images ×800 for all panels. The images are representative of three independent preparations. (B) Graphical representation of immunofluorescence confocal microscopy. Data are mean ± SEM (n=3). All data are representative of three independent experiments; all are presented as mean ± SD. P values were determined by Student's t-test; *$p < 0.05$, **$p < 0.005$.

3.8. Antimicrobial assays

Therapeutics of a novel drug is important as it should show dual activity for anti-inflammatory and anti-bacterial activity. The expression of pro-inflammatory cytokines and expression of phosphor-TIRAP through confocal microscopy has been done. For the anti-microbial activity, Growth profile of polymicrobial culture against presence of different concentration

of drug 5 has been done. Antimicrobial assay was initially carried out by disc diffusion method followed by broth dilution assay. Drug 5 showed a clear zone of inhibition against polymicrobial organisms. It exerted zones of inhibition of 16±2 and 23±2 mm respectively against mixed culture and which indicates higher efficacy of the drug 5 against mixed culture (**Figure:3.11.**)

The antimicrobial activity of drug 5 was further confirmed by the determination of respective MIC and MBC values against the test organisms by broth dilution assay. The MIC is the lowest concentration of antimicrobial agents that completely visually inhibits the growth of the microorganisms while MBC is defined as the lowest concentration of antimicrobial agent that kills 99.9% of the initial bacterial population. For growth inhibitory concentration (≥MIC), the presence of viable microorganisms was tested and the lowest concentration causing bactericidal effect was reported as MBC. The drug 5 exerted MIC value of 40 μg against mixed culture of gram negative as well as gram positive culture. Whereas MBC values of 60 μg. Both the MIC and MBC values of drug 5 against the microbial culture show that drug 5 might exert anti-microbial activity.

(a)

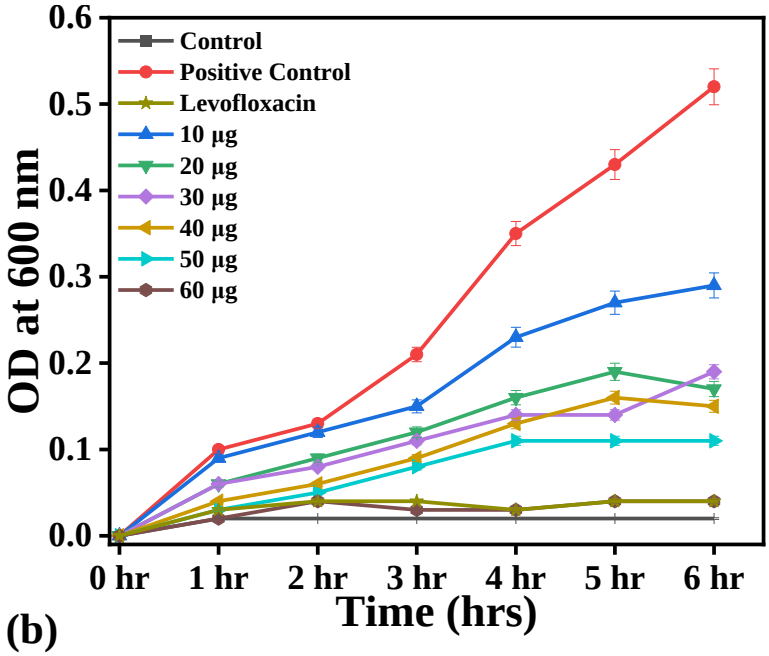
Control
Positive Control
Levofloxacin
10 µg
20 µg
30 µg
40 µg
50 µg
60 µg
OD at 600 nm
0.0
0.1
0.2
0.3
0.4
0.5
0.6
0 hr
1 hr
2 hr
3 hr
4 hr
5 hr
6 hr
Time (hrs)

(b)

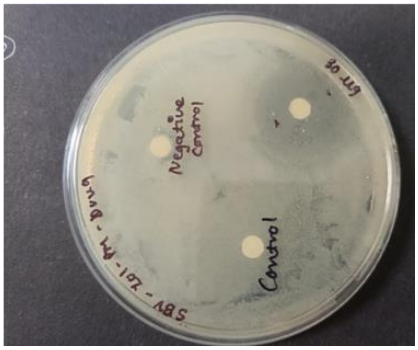
Negative Control
Control

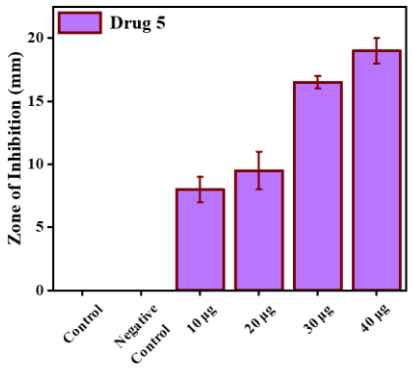
Drug 5
Zone of Inhibition (mm)
0
5
10
15
20
Control
Negative Control
10 µg
20 µg
30 µg
40 µg

Figure: 3.11. (A) Growth profile analysis of polymicrobial culture against different concentration from 10 μg to 60 μg and incubated for 12 -24 hours. Here, data represents incubation of 6 hours. In positive culture, bacterial density increases while the higher concentration of drug shows no more increase in bacterial density. (B) Zone of inhibition of drug against polymicrobial culture at different drug concentration. Data are mean ± SEM (n=3). All data are representative of three independent experiments; all are presented as mean ± SD. P values were determined by Student's t-test; *$p < 0.05$, **$p < 0.005$.

Chapter: 4

Conclusion and Future aspects

Sepsis is a chronic inflammatory disease that is a major cause of morbidity and mortality, it can lead to organ failure and disruption and eventually to death. Currently, therapeutics is only based on some antibiotics and steroidal drug molecules, and the mortality rate is still 40-80 %. Along with this the emergence of antibiotic resistance makes it vulnerable to treat the sepsis condition. So, there is need of developing a potent therapeutic strategy which can target both the aspects of killing the pathogens as well as the dysregulated host immune response.

This study aims to develop a therapeutic drug which can meet both aspects. A novel drug molecule will show the dual activity targeting the specific bacterial target and inflammatory target. Recent studies reported that levofloxacin- a broad range antibiotic shows dual activity-Anti-bacterial and Anti-inflammatory activity. The emergence of antimicrobial resistance lowers the efficacy of levofloxacin. The discovery of new antibiotics or drug molecules is very important which shows both the activities as well as efficacy against pathogenic resistance microbes. In this context, we screened levofloxacin similar 3D conformers against DNA Gyrase and TIRAP protein. Computational studies were conducted and finalized the five drug molecules. *In vitro* studies were done to check whether this drug 5 molecule has anti-inflammatory activity based on the expression of pro-inflammatory cytokines, and expression of phosphorylation of TIRAP. Cell cytotoxicity assay was performed which suggest that drug 5 was not toxic up to 100 µM through MTT assay and Hemolysis assay.

Drug 5 (D5) showing dual activities will be confirmed by western blotting and further *in vivo* experiments. In Future aspects, we wanted to study either this drug showing efficacy towards anti-microbial resistant pathogens or not. We have already started studies regarding AMR and have sent drug to pathogenic microbiology lab for further experiments.

Chapter: 5

Annexure

5.1. List of primers

Table 5.1: Primer sets used for RT-PCR

S.No.	Gene target	Sequence (5'-3')
1.	GAPDH (F)	AACTTTGGCATTGTGGAAGG
2.	GAPDH (R)	CACATTGGGGGTAGGAACAC
3.	IL-1β (F)	TGCCACCTTTTGACAGTGATG
4.	IL-1β (R)	AAGGTCCACGGGAAAGACAC
5.	IL-6 (F)	GCCTTCTTGGGACTGATGCT
6.	IL-6 (R)	TGCCATTGCACAACTCTTTTC
7.	TNFα (F)	AGGCACTCCCCCAAAAGATG
8.	TNFα (R)	CCACTTGGTGGTTTGTGAGTG

5.2. List of antibodies

Table 5.2: Antibodies used for immunofluorescence.

S. No.	Antibody	Cat. No.	Dilution used for immunofluorescence
1.	p-TIRAP	BS-756R	(1:200)
2.	TIRAP	13077S	(1:200)
3.	Anti-Mouse HRP	Sc-2318	(1:1000)
4.	Anti-Rabbit-AF594	A11012	(1;1000)
5.	p65	Sc-8008	(1:200)
6.	p-p65	CS-3033	(1:200)

References

Anderson, V. & Osheroff, N., 2001, 'Type II Topoisomerases as Targets for Quinolone Antibacterials Turning Dr. Jekyll into Mr. Hyde', *Current Pharmaceutical Design*, 7(5), 337–353.

Belhaouane, I., Hoffmann, E., Chamaillard, M., Brodin, P. & Machelart, A., 2020, 'Paradoxical Roles of the MAL/Tirap Adaptor in Pathologies', *Frontiers in Immunology*, 11, 569127.

Boyd, N.K., Lee, G.C., Teng, C. & Frei, C.R., 2021, 'In vitro activity of non-antibiotic drugs against Staphylococcus aureus clinical strains', *Journal of Global Antimicrobial Resistance*, 27, 167–171.

Champoux, J.J., 2001, 'DNA Topoisomerases: Structure, Function, and Mechanism', *Annual Review of Biochemistry*, 70(1), 369–413.

Chen, L., Deng, H., Cui, H., Fang, J., Zuo, Z., Deng, J., Li, Y., Wang, X. & Zhao, L., 2018, 'Inflammatory responses and inflammation-associated diseases in organs', *Oncotarget*, 9(6), 7204–7218.

Cho, K., Joannopoulos, J.D. & Kleinman, L., 1993, 'Constant-temperature molecular dynamics with momentum conservation', *Physical Review E*, 47(5), 3145–3151.

Chopra, S., Matsuyama, K., Tran, T., Malerich, J.P., Wan, B., Franzblau, S.G., Lun, S., Guo, H., Maiga, M.C., Bishai, W.R. & Madrid, P.B., 2012, 'Evaluation of gyrase B as a drug target in Mycobacterium tuberculosis', *Journal of Antimicrobial Chemotherapy*, 67(2), 415–421.

Cozzarelli, N.R., 1980, 'DNA Gyrase and the Supercoiling of DNA', *Science*, 207(4434), 953–960.

Deguine, J. & Barton, G.M., 2014, 'MyD88: a central player in innate immune signaling', *F1000Prime Reports*, 6.

Dighe, S.N. & Collet, T.A., 2020, 'Recent advances in DNA gyrase-targeted antimicrobial agents', *European Journal of Medicinal Chemistry*, 199, 112326.

Duque-Villegas, M.A., Abbadi, B.L., Romero, P.R., Galina, L., Dalberto, P.F., Rodrigues-Junior, V.D.S., Roth, C.D., Rambo, R.S., Vieira De Souza, E., Perello, M.A., Machado, P., Basso, L.A. & Bizarro, C.V., 2020, *Evaluating* aroA *gene essentiality and EPSP synthase*

vulnerability in Mycobacterium smegmatis *under different nutritional conditions*.

Gyawali, B., Ramakrishna, K. & Dhamoon, A.S., 2019, 'Sepsis: The evolution in definition, pathophysiology, and management', *SAGE Open Medicine*, 7, 205031211983504.

Handoko, S.D., Xuchang Ouyang, Chinh Tran To Su, Chee Keong Kwoh, & Yew Soon Ong, 2012, 'QuickVina: Accelerating AutoDock Vina Using Gradient-Based Heuristics for Global Optimization', *IEEE/ACM Transactions on Computational Biology and Bioinformatics*, 9(5), 1266–1272.

Hoover, W.G., 1985, 'Canonical dynamics: Equilibrium phase-space distributions', *Physical Review A*, 31(3), 1695–1697.

Huang, M., Cai, S. & Su, J., 2019, 'The Pathogenesis of Sepsis and Potential Therapeutic Targets', *International Journal of Molecular Sciences*, 20(21), 5376.

Lannoy, V., Côté-Biron, A., Asselin, C. & Rivard, N., 2023, 'TIRAP, TRAM, and Toll-Like Receptors: The Untold Story', G. Xu (ed.), *Mediators of Inflammation*, 2023, 1–13.

Leekha, S., Terrell, C.L. & Edson, R.S., 2011, 'General Principles of Antimicrobial Therapy', *Mayo Clinic Proceedings*, 86(2), 156–167.

Loots, F.J., Smulders, D., Giesen, P., Hopstaken, R.M. & Smits, M., 2021, 'Vital signs of the systemic inflammatory response syndrome in adult patients with acute infections presenting in out-of-hours primary care: A cross-sectional study', *European Journal of General Practice*, 27(1), 83–89.

Lu, C., Wu, C., Ghoreishi, D., Chen, W., Wang, L., Damm, W., Ross, G.A., Dahlgren, M.K., Russell, E., Von Bargen, C.D., Abel, R., Friesner, R.A. & Harder, E.D., 2021, 'OPLS4: Improving Force Field Accuracy on Challenging Regimes of Chemical Space', *Journal of Chemical Theory and Computation*, 17(7), 4291–4300.

Lyne, P.D., Lamb, M.L. & Saeh, J.C., 2006, 'Accurate Prediction of the Relative Potencies of Members of a Series of Kinase Inhibitors Using Molecular Docking and MM-GBSA Scoring', *Journal of Medicinal Chemistry*, 49(16), 4805–4808.

Madhavi Sastry, G., Adzhigirey, M., Day, T., Annabhimoju, R. & Sherman, W., 2013, 'Protein and ligand preparation: parameters, protocols, and influence on virtual screening enrichments', *Journal of Computer-Aided Molecular Design*, 27(3), 221–234.

Martin, G.S., 2012, 'Sepsis, severe sepsis and septic shock: changes in incidence, pathogens and outcomes', *Expert Review of Anti-infective Therapy*, 10(6), 701–706.

McKie, S.J., Neuman, K.C. & Maxwell, A., 2021, 'DNA topoisomerases: Advances in understanding of cellular roles and multi-protein complexes via structure-function analysis', *BioEssays*, 43(4), 2000286.

Morris, G.M., Huey, R., Lindstrom, W., Sanner, M.F., Belew, R.K., Goodsell, D.S. & Olson, A.J., 2009, 'AutoDock4 and AutoDockTools4: Automated docking with selective receptor flexibility', *Journal of Computational Chemistry*, 30(16), 2785–2791.

Nedeva, C., Menassa, J. & Puthalakath, H., 2019, 'Sepsis: Inflammation Is a Necessary Evil', *Frontiers in Cell and Developmental Biology*, 7, 108.

Nosé, S., 1984, 'A unified formulation of the constant temperature molecular dynamics methods', *The Journal of Chemical Physics*, 81(1), 511–519.

Onseedaeng, S. & Ratthawongjirakul, P., 2016, 'Rapid Detection of Genomic Mutations in *gyrA* and *parC* Genes of *Escherichia coli* by Multiplex Allele Specific Polymerase Chain Reaction', *Journal of Clinical Laboratory Analysis*, 30(6), 947–955.

Pawar, A., Raut, A., Kalrao, V., Jacob, J., Godha, I. & Thomas, R., 2016, 'Etiology and Clinical Outcomes of Neonatal and Pediatric Sepsis', *Archives of Pediatric Infectious Diseases*, 4(2).

Rajpoot, S., Wary, K.K., Ibbott, R., Liu, D., Saqib, U., Thurston, T.L.M. & Baig, M.S., 2021, 'TIRAP in the Mechanism of Inflammation', *Frontiers in Immunology*, 12, 697588.

Rudd, K.E., Kissoon, N., Limmathurotsakul, D., Bory, S., Mutahunga, B., Seymour, C.W., Angus, D.C. & West, T.E., 2018, 'The global burden of sepsis: barriers and potential solutions', *Critical Care*, 22(1), 232.

Spencer, A.C. & Panda, S.S., 2023, 'DNA Gyrase as a Target for Quinolones', *Biomedicines*, 11(2), 371.

Sygitowicz, G. & Sitkiewicz, D., 2020, 'Molecular mechanisms of organ damage in sepsis: an overview', *The Brazilian Journal of Infectious Diseases*, 24(6), 552–560.

Tsalamandris, S., Antonopoulos, A.S., Oikonomou, E., Papamikroulis, G.-A., Vogiatzi, G., Papaioannou, S., Deftereos, S. & Tousoulis, D., 2019, 'The Role of Inflammation in Diabetes: Current Concepts and Future Perspectives', *European Cardiology Review*, 14(1), 50–59.

Wohlkonig, A., Chan, P.F., Fosberry, A.P., Homes, P., Huang, J., Kranz, M., Leydon, V.R., Miles, T.J., Pearson, N.D., Perera, R.L., Shillings, A.J., Gwynn, M.N. & Bax, B.D., 2010, 'Structural basis of quinolone inhibition of type IIA topoisomerases and target-mediated resistance', *Nature Structural & Molecular Biology*, 17(9), 1152–1153.